Evaluating The Sensitivity and Applicability of Precipitation-Based and Precipitation-Evapotranspiration-Based Drought Indices To Different Record Periods

Liang Li
Northwest A&F University: Northwest Agriculture and Forestry University
Hong He
Northwest A&F University: Northwest Agriculture and Forestry University
Qiaojuan Wang
Northwest A&F University: Northwest Agriculture and Forestry University
Xiaoyun Wang
Northwest A&F University: Northwest Agriculture and Forestry University
Yuxin Cao
Northwest A&F University: Northwest Agriculture and Forestry University
Huanjie Cai (huanjiec@yahoo.com)
Key Laboratory of Agricultural Soil and Water Engineering in Arid and Semiarid of Ministry of Education, Northwest A&F University, Yangling, Shaanxi 712100, China

Research Article

Keywords: Sensitivity, Applicability, Precipitation-based drought indices, Precipitation-evapotranspiration-based drought indices, Record periods

Posted Date: October 1st, 2021

DOI: https://doi.org/10.21203/rs.3.rs-896277/v1

Evaluating the sensitivity and applicability of precipitation-based and precipitation-evapotranspiration-based drought indices to different record periods

Authors: Liang Li [a,b,c], Hong He [a,b,c], Qiaojuan Wang [a,b,c], Xiaoyun Wang [a,b,c], Yuxin Cao [a,b,c], Huanjie Cai [a,b,c*]

[a] Key Laboratory of Agricultural Soil and Water Engineering in Arid and Semiarid Areas, Ministry of Education, Northwest A&F University, Yangling, 712100, China

[b] Institute of Water-saving Agriculture in Arid Areas of China, Northwest A&F University, Yangling, 712100, China

[c] College of Water Resources and Architectural Engineering, Northwest A&F University, Yangling, 712100, China

[*]**Corresponding author:** Huanjie Cai. Mailing address: No.23 Weihui Road, Yangling, Shaanxi Province, 712100, P. R. China; Tel: +86-(0)29-87082133; E-mail: huanjiec@yahoo.com

Abstract

As drought indices are generally calculated based on multi-year historical data spanning periods of at least 30 years, different drought index values at certain times are therefore calculated due to different record lengths, making it difficult to accurately define dry or wet periods in a studied region or station. This investigation assessed the sensitivity and applicability of precipitation-based and precipitation-evapotranspiration-based drought indices, such as the Generalized extreme value drought index (GEVI), Homogeneity index of precipitation and temperature (HI), the K index (K), Precipitation anomaly percentage (Pa), Standardized precipitation evapotranspiration index (SPEI), Standardized precipitation index (SPI), and the China Z index (CZI), to different record lengths on monthly, seasonal and annual time scales. By using monthly, seasonal and annual precipitation and evapotranspiration data from a research station over the period 1961-2017, data over periods of 55, 50, 45, 40, 35 and 30 years were extracted. Analysis of correlation coefficient of all indices, match and non-match, and actual drought and no-drought recognition rate of the indices indicated that K, Pa and SPEI indices recorded better time stability compared to other indices at all time scales across different climatic zones in the study region; the GEVI index recorded the lowest time stability compared to other indices. Results also indicated that the majority of optimal lengths for all stations having the lowest non-match were 41-45 years, with some indices at different time scales being 36-40 years and 46-50 years. In addition, the HI index had the highest actual drought and no-drought recognition rate at almost all climate zones, followed by Pa and SPEI indices. Results from this study indicate that more priority should be given to precipitation-evapotranspiration-based indices when studying a large region; indices with concrete results should be selected when analyzing relatively small regions.

Keywords: Sensitivity; Applicability; Precipitation-based drought indices; Precipitation-evapotranspiration-based drought indices; Record periods

Declarations

Ethics approval and consent to participate

Not applicable.

Consent for publication

Not applicable.

Availability of data and materials

The datasets used and/or analysed during the current study are available from the corresponding author on reasonable request.

Competing interests

We declare that we have no financial and personal relationships with other people or organizations that can inappropriately influence our work, there is no professional or other personal interest of any nature or kind in any product, service and/or company that could be construed as influencing the position presented in, or the review of, the manuscript entitled.

Funding

This study was supported by the National Natural Science Foundation of China (Grant No.51879223) and the National Key Research and Development Program of China (Grant No.2016YFC0400201) to obtain study data.

Authors' contributions

Liang Li analyzed and interpreted the study data, and wrote the manuscript. Hone He calculated and analyzed the study data. Qiaojuan Wang calculated the study data. Xiaoyun Wang calculated the study data. Yuxin Cao modified the manuscript. Huanjie Cai modified the manuscript and provided the fundings. All authors read and approved the final manuscript.

1. Introduction

As drought episodes can occur in high as well as low rainfall areas over an extended period of time, this natural disaster is one of the most complex hydroclimatic disasters occurring in the world (Mishra and Singh, 2010; Vicente-Serrano et al., 2019). This phenomenon has the greatest effect on human activities compared to other natural hazards (Freire-González et al., 2017; Keyantash and Dracup, 2002; Lopez-Nicolas et al., 2017). Drought characteristics are distinguished from other water-related natural disasters, whose effects are basically non-structural with a wide spatial extent, as well as causing significant levels of damage (Mahmoudi et al., 2019). Although planning and management of water resources pay special attention to possible drought episodes, it is very difficult to monitor droughts due to their complex features (Makokha et al., 2016).

Although almost all climatic regions in the world have suffered from drought episodes, with drought effects being more serious in arid and semi-arid regimes (Valverde-Arias et al., 2017). It is therefore vital in these areas that planners define the characteristics of droughts and wet periods for water resource management. The arid area of Northwest China is one of the most vulnerable arid and semi-arid regions of the world. This area is characterized by relatively low precipitation levels, high changes in the rate of precipitation, and uneven spatial and temporal distribution of precipitation (Geng et al., 2014). In recent years, severe regional drought episodes have become more frequent under a changing climate, episodes which are likely to increase in frequency for the foreseeable future (Jia et al., 2018). Precipitation anomalies have also increased in arid areas of Northwest China due to global climate change, resulting in more complicated temporal-spatial properties in these arid areas (Zhang et al., 2017; Zhao et al., 2017), leading to an increase in economic, social and bioenvironmental damage.

It is therefore important to identify a set of appropriate and accurate indices to quantify and evaluate drought severity, duration and range in certain regions. To date, a number of drought indices have been defined

in various areas of the world, all of which are based on climatic and environmental data, including the Palmer Drought Severity Index (PDSI; Palmer, 1965), the Standardized Precipitation Index (SPI; McKee et al., 1993), the Standardized Precipitation Evapotranspiration Index (SPEI; Vicente-Serrano et al., 2010) and the China-Z Index (CZI; Dogan et al., 2012). These indices can be used to formulate drought-resisting measures and policies.

Due to different research aims and different study regions, more and more indices for drought monitoring have been being defined, resulting in an increase in comparative studies on different drought indices and their applicability in different regions. By comparing the applicability of different drought indices, researchers can choose the best index to monitor drought episodes in a study region in terms of their research aim. In order to evaluate drought indices' dependability and effectiveness in determining the severity and evolution of droughts, Dogan et al. (2012) selected seven drought precipitation-based indices to determine the effect of timestep for choosing an appropriate value and the sensitivity of drought indices to timestep and choice of a drought index. Results from this investigation concluded that the Effective Drought Index (EDI) was more sensitive to monthly rainfall changes in terms of multi-monthly cumulative rainfall changes; this index also had the best correlation with other drought indices. Mercado et al. (2016) also compared the variation and performance of seven drought indices to identify droughts using Non-Contiguous Drought Analysis. They concluded that to identify drought events and drought spatio-temporal evolution, it was important to combine different drought indices, meteorological, hydrological and agricultural drought indices by analyzing drought evolution, severity and trends in mainland China using four drought indices. Yao et al. (2017) revealed that all indices were regional- or station-specific. Kassaye et al. (2020) examined the evolution of drought episodes in Ethiopia using four drought indices, recording that SPI and SPEI had a stronger correlation than SPI and China Z Index (CZI) at all time scales.

Among drought indices currently used, PDSI is generally the most used index (Ma et al., 2014). However, this index is very complex. It has empirical derivation, and it requires multiple types of data, resulting in this index having numerous problems, giving it low practicability as an accurate index (Kim et al., 2009; Liu et al., 2016; Nam et al., 2015). In light of this, SPI was formulated by McKee et al. (1993) to provide a better, easier and more accurate index to monitor droughts and wetness. SPI can be calculated at different time intervals or time scales, and it has been widely used as an appropriate tool to analyze precipitation and regional droughts, as well as local droughts around the world (Amirataee et al., 2017; Lei et al., 2020; Mallya et al., 2016; Nam et al., 2015; Quesada-Hernández et al., 2019; Ribeiro and Pires, 2016; Stagge et al., 2015). Despite the advantages SPI affords, it has some limitations. For example, SPI can produce false results due to a single day of heavy rainfall in the monitoring period - this index can classify a month as being wet even though all days bar one very wet day were rainless (Wu et al., 2015). In addition, SPI does not take the balance between precipitation and evaporation (the water balance) into consideration (Adnan et al., 2017; Chang et al., 2016; Homdee et al., 2016; Touma et al., 2015).

In order to overcome these limitations, SPEI was developed by Vicente-Serrano et al. (2015). This index considers the water balance calculated by the difference between precipitation and evapotranspiration, making it more suitable to quantify drought. Due to its simple interpretation, low data requirements which satisfy most climate data products, and its multiscalar flexibility, this index has quickly become popular. These characteristics allow users to evaluate drought events in terms of different purposes, such as agricultural, hydrological, and socioeconomic, enabling monitoring by calculating different accumulation periods of the indices. This index has been applied in different environments globally (Afzal and Ragab, 2020; Ahmadalipour et al., 2017; Alam et al., 2017; Ayantobo et al., 2017; Hao et al., 2015; Homdee et al., 2016; Hui-Mean et al.,

2018; Lu et al., 2020; Mallya et al., 2016; Nam et al., 2015; Peña-Gallardo et al., 2019; Spinoni et al., 2017; Su et al., 2018; Wang et al., 2020; Zhou et al., 2020).

The aforementioned indices, however, also have several limitations and disadvantages. One limitation is the sensitivity of the index to the probability distributions used on it, with the distribution possibly not being appropriate for all investigated regions. For example, Mallya et al. (2015) employed the gamma mixture model (Gamma-MM) in a Bayesian framework to alleviate the choice of a suitable distribution for fitting data in SPI. Another disadvantage is that the index may be sensitive to the length of the examined record, thereby limiting the use of the index at different regions where only short-term data is available. As drought indices are generally calculated based on multi-year historical data, different drought index values are therefore calculated at a certain time due to the different record lengths used. For example, one drought index value may be classified from wetness to drought or from drought to wetness if the value was calculated using two different record lengths in terms of a certain drought index, thereby causing difficulty in setting the studied region or station to either being dry or wet. Wu et al. (2005) analyzed the effect record length had on SPI by examining correlation coefficients, the index of agreement, and the consistency of dry/wet event categories. Results indicated that SPI values computed from different record lengths were highly correlated and consistent at different time periods. Mahmoudi et al. (2019) also evaluated the sensitivity of seven precipitation-based drought indices to different record lengths, finding that EDI was the most stable index in their study region.

Previous investigations have highlighted that two weak points in the applied indices are sensitivity and applicability of the indices based on precipitation and evapotranspiration in relation to the length of the various temporal periods in different climatic regions. Although it is important to consider other indices and other regions, Mahmoudi et al. (2019) considered seven drought indices as well as only examining precipitation-based

drought indices. In this investigation, therefore, we assess the sensitivity and applicability of precipitation-based and precipitation-evapotranspiration-based drought indices (GEVI, HI, K, Pa, SPEI, SPI, and CZI) to different record lengths to select a regional applicable drought index.

2. Study area and data

The arid region of Northwest China was selected as the study area for this investigation. This region is characterized by specific geographical and topographical characteristics, (Geng et al., 2014), resulting in different climatic regimes. Based on previous classification (Huang, 1958) and data from the Resource and Environment Science and Data Center (https://www.resdc.cn/Default.aspx), arid areas in Northwest China can be divided into ten climatic regions (Figure 1), which were characterized by accumulated temperature and moisture index. The whole area was initially divided into different temperature zones by accumulated temperature: mid-temperate zone (1700-3500℃), warm temperate zone (3500-4500℃), North subtropical zone (4500-5300℃), plateau temperate zone (1500-3000℃), plateau sub-cold zone (500-1500℃) and plateau cold zone (0-500℃). The area was then divided into different humidity zones by annual precipitation (P) and humidity degree (the relationship between precipitation and evaporation (E)): wet zone (P>800 mm, P>E), semi-humid zone (P>400 mm, P>E), semi-arid zone (P<400 mm, P<E) and arid zone (P<200 mm, P<E). Meteorology data used in this study was derived from the China Meteorological Data Service Centre (http://data.cma.cn/en). In this study, one station representing a climate region was selected, except for two zones whose meteorological stations were little sited. Therefore, eight meteorological stations were selected in this study to investigate specific characteristics in the different regions.

In this study, monthly, seasonal and annual precipitation data were used from a 57-year period (1961-2017). The names, geographical coordinates, mean annual temperatures, total means of annual precipitation,

167 establishment years and types of station used are recorded in Table 1. Record lengths of 55, 50, 45, 40, 35 and
168 30 years were extracted from the main period (1961-2017) for monthly, seasonal and annual time scales.

169 **3. Methodology**

170 The method used in this study was derived from research undertaken by Wu et al. (2005), where impact
171 lengths of data records were examined using SPI values. In this investigation, drought indices were calculated
172 using Python software for set time scales for all selected record lengths. Indices used in this study are also
173 briefly introduced.

174 3.1. Generalized extreme value drought index (GEVI)

175 GEVI assumes precipitation series as a generalized extreme value distribution function, based on
176 precipitation relative hydrological variables skewed to the right (Wang et al., 2013). The probability distribution
177 function of the GEVI series is:

178 $$f(x)=\frac{1}{v}e^{[-(1-w)y-e^{(-y)}]} \tag{1}$$

179 where,

180 $$y=\begin{cases}\dfrac{x-u}{v} & w=0\\ -\dfrac{1}{w}\ln[1-\dfrac{w(x-u)}{v}] & w\neq 0\end{cases} \tag{2}$$

181 The cumulative distribution function of the generalized extreme value is:

182 $$F(x)=e^{e^{(-y)}}=\begin{cases}e^{\{-[1+w(\frac{x-u}{v})]^{-\frac{1}{w}}\}} & w\neq 0\\ e^{\{-e^{[-(\frac{x-u}{v})]}\}} & w=0\end{cases} \tag{3}$$

183 The corresponding inverse function for a given frequency F was then solved as:

184 $$x_F=\begin{cases}u+v\{1-[\ln(F)]^w/w\} & w\neq 0\\ u-v\ln[-\ln(F)] & w=0\end{cases} \tag{4}$$

where, x is precipitation at a certain period; and u, v, w are location, scale and shape parameters of GEVI probability distribution, respectively. Values were estimated using marimum likelihood, linear moments and maximum product of spacing, respectively.

GEVI is therefore defined as a complex negative logarithm of $F(x)$ as the drought index:

$$\mathrm{GEVI} = -\ln(-\ln(F)] = -\frac{1}{w}\ln[1-\frac{w(x_i-u)}{v}] \tag{5}$$

where, GEVI is the drought index; and x_i is precipitation at a certain timescale.

3.2. Homogeneity index of precipitation and temperature (HI)

The HI of precipitation and temperature takes precipitation and temperature into consideration, providing a quick response to precipitation and temperature changes. This index is defined as (Wu et al., 2011):

$$\mathrm{HI}=\frac{P-\bar{P}}{\sigma P}-\frac{T-\bar{T}}{\sigma T} \tag{6}$$

where, HI is the Homogeneity index of precipitation and temperature; P is precipitation at a certain timescale; $\bar{P}$ is mean precipitation at a certain period; σP is mean square error of precipitation; T is temperature at a certain timescale; T is mean temperature at a certain period; and σT is the mean square error of temperature.

3.3. The K index (K)

The K drought index takes precipitation and ET0 into consideration, defined as (Wu et al., 2012):

$$K_{ij} = P'_{ij} / E'_{ij} \tag{7}$$

$$P'_{ij} = P_{ij} / \bar{P}_i \tag{8}$$

$$E'_{ij} = E_{ij} / \bar{E}_i \tag{9}$$

where, K_{ij} is the K drought index at a certain time; P'_{ij} is the relative change rate of precipitation at a certain period; E'_{ij} is the relative change rate of ET0 at a certain period; P_{ij} is precipitation at a certain time; $\bar{P}_i$ is

mean precipitation at a certain period; E_{ij} is ET0 at a certain time period; and $\overline{E}_i$ is mean ET0 at a certain period; i = 1, 2, …, n, is timescale, month; j = 1, 2, …, m, is the station number.

3.4. Precipitation anomaly percentage (Pa)

Precipitation anomaly percentage reflects the degree of deviation between precipitation in a certain period and the contemporaneous mean state, defined as (Wei and Ma, 2003):

$$Pa = \frac{P - \overline{P}}{\overline{P}} \times 100\% \tag{10}$$

where, P is precipitation in a certain period; and $\overline{P}$ is contemporaneous mean precipitation, calculated as:

$$\overline{P} = \frac{1}{n}\sum_{i=1}^{n} P_i \tag{11}$$

3.5. Standardized precipitation evapotranspiration index (SPEI)

This index, proposed by Vicente-Serrano et al. (2010), uses the moisture deficit (D) between precipitation (P) and ET0 to track the water balance to recognize dryness and wetness. Here, $D_i = P_i - ET0_i$, where i represents the i-th month. D_i is normalized with a log-logistic probability distribution to obtain SPEI, calculated as (Begueria et al., 2014; Vicente-Serrano et al., 2010; Xu et al., 2015):

$$f(x) = \frac{\beta}{\alpha}\left(\frac{x-\gamma}{\alpha}\right)^{\beta-1}\left[1+\left(\frac{x-\gamma}{\alpha}\right)^{\beta}\right]^{-2} \tag{12}$$

$$F(x) = \int_0^x f(x)dt = \left[1+\left(\frac{\alpha}{x-\gamma}\right)^{\beta}\right]^{-1} \tag{13}$$

where, α, β, γ are scale, shape and location parameters, respectively. These parameters are calculated as:

$$\alpha = \frac{(W_0 - 2W_1)\beta}{\Gamma(1+1/\beta)\Gamma(1-1/\beta)} \tag{14}$$

$$\beta = \frac{2W_1 - W_0}{6W_1 - W_0 - 6W_2} \tag{15}$$

$$\gamma = W_0 - \alpha\Gamma(1+1/\beta)\Gamma(1-1/\beta) \tag{16}$$

where, Γ is gamma function; and W_0, W_1, W_2 are probability weighted moments of original sequences D_i:

$$W_s = \frac{1}{N}\sum_{i=1}^{N}(1-F_i)^S D_i \tag{17}$$

$$F_i = \frac{i - 0.35}{N} \tag{18}$$

where, N is the number of calculating D_i; and i is the ordinal of D_i in ascending order.

SPEI can then be transformed into the standardized value of $F(x)$, as:

$$SPEI = S(W - \frac{C_0 + C_1 W + C_2 W^2}{1 + d_1 W + d_2 W^2 + d_3 W^3}) \tag{19}$$

$$W = \begin{cases} \sqrt{-2\ln(1 - F(x))} & 0.5 \le F(x) \le 1.0 \\ -2\ln F(x) & 0 < F < 0.5 \end{cases} \tag{20}$$

$$S = \begin{cases} 1 & 0.5 \le F(x) \le 1.0 \\ -1 & 0 < F(x) < 0.5 \end{cases} \tag{21}$$

In addition, c_0, c_1, c_2, d_1, d_2, d_3 are constant coefficients as follows:

$$c_0 = 2.515517, c_1 = 0.802853, c_2 = 0.010328; d_1 = 1.432788, d_2 = 0.189269, d_3 = 0.001308.$$

3.6. Standardized precipitation index (SPI)

This index, proposed by McKee et al. (1993), is based only on the precipitation variable and it can recognize the drought phenomena in different regions. The index set gamma family functions for fit to precipitation data, defined as:

$$f(x) = \frac{1}{\beta^{\gamma}\Gamma(\gamma)} x^{\gamma - 1} e^{-x/\beta} \tag{22}$$

where, $\gamma > 0$, shape parameter; $\beta > 0$, scale parameter; x is the precipitation amount; and $\Gamma(\gamma)$ is the gamma function. Parameters are estimated using the maximum likelihood method, as:

$$\hat{\gamma} = \frac{1 + \sqrt{1 + 4A/3}}{4A} \tag{23}$$

$$\hat{\beta} = \frac{\overline{x}}{\hat{\gamma}} \tag{24}$$

$$A = \ln \overline{x} - \frac{1}{n}\sum_{i=1}^{n} \ln x_i \tag{25}$$

where, n is the number of precipitation data. Assuming $t = x / \hat{\beta}$, the cumulative probability is transformed into the incomplete gamma function, as:

$$G(x) = \int_0^x y(x)dx = \frac{1}{\beta^{\gamma}\Gamma(\gamma)}\int_0^x x^{\gamma-1}e^{-x/\beta}dx \quad (26)$$

When the gamma function is not defined for x=0 and precipitation distribution is 0, the cumulative probability is calculated as:

$$H(x) = q + (1-q)G(x) \quad (27)$$

In Equation 27, the precipitation probability is 0, while m is the number of zeros in the precipitation time series. q is estimated in m/n and $H(x)$ is transformed into variable (Z) with the following approximation:

$$SPI = Z = S\{t - \frac{(c_2t + c_1)t + c_0}{[(d_3t + d_2)t + d_1]t + 1.0}\} \quad (28)$$

where:

$$S = \begin{cases} 1 & H(x) > 0.5 \\ -1 & H(x) \le 0.5 \end{cases} \quad (29)$$

$$t = \sqrt{\ln\frac{1}{F^2}} \quad (30)$$

$$F = \begin{cases} 1.0 - H(x) & H(x) > 0.5 \\ H(x) & H(x) \le 0.5 \end{cases} \quad (31)$$

In addition, c_0, c_1, c_2, d_1, d_2, d_3 are constant coefficients as follows:

$$c_0 = 2.515517, c_1 = 0.802853, c_2 = 0.010328; d_1 = 1.432788, d_2 = 0.189269, d_3 = 0.001308.$$

3.7. The China Z index (CZI)

CZI was widely used in 1995 by the National Climate Center of China. This index was used with the assumption that the data followed the Pearson Type Ⅲ distribution, defined as (Ma et al., 2013):

$$f(x) = \frac{\beta}{\Gamma(\alpha)}(x-\alpha)^{\alpha-1}e^{-\beta(x-\alpha)}, (x > \alpha) \quad (32)$$

Precipitation is then normalized into a standardized normal distribution as:

$$Z_i = \frac{6}{C_s}\left|\frac{C_s}{2}\Phi_i + 1\right|^{\frac{1}{3}} - \frac{6}{C_s} \quad (33)$$

where, C_s is the coefficient of skew; and Φ_i is the standard variable, defined as:

$$C_s = \frac{\sum_{i=1}^{n}(X_i - X)^3}{n\sigma^3} \quad (34)$$

$$\Phi_i = \frac{X_i - X}{\sigma} \quad (35)$$

σ and X are defined as:

$$\sigma = \sqrt{\frac{1}{n}\sum_{i=1}^{n}(X_i - X)^2} \quad (36)$$

$$X = \frac{1}{n}\sum_{i=1}^{n} X_i \quad (37)$$

4. Results and discussion

Seven drought indices of GEVI, HI, K, Pa, SPEI, SPI and CZI were initially used in conjunction with record lengths from 57 to 30 years (on a yearly basis) to calculate drought indices on monthly, seasonal and annual time scales. The sensitivity of the record lengths was then investigated using several steps. The correlation coefficient of all indices, and the match and non-match of the indices obtained from all record lengths (28) were determined and analyzed for each time scale. Results provided a 28×28 matrix for correlation coefficient and non-match of the indices at each time scale. Optimal record lengths were also recorded by analyzing the maximum average correlation coefficient of all indices at the three time scales, providing the opportunity to monitor drought episodes of the different indices at different time scales. Finally, we compared actual drought and no-drought recognition rates of different indices on a seasonal time scale to verify the applicability of the drought indices.

4.1. Comparison of correlation coefficients

Spearman correlation coefficient (rank) and Pearson correlation coefficient were obtained for all stations on monthly, seasonal and annual time scales; 2-3 cases from each time scale were included in the study. As the

results of two correlation coefficients were very close and similar to each other, the results of the Spearman correlation coefficient were also included in our analysis.

Firstly, as the recorded length of the indices increased, the overall correlation coefficient between record lengths initially increased before decreasing. This indicates a variation trend in the quadratic polynomial, and its whole linear trend was increasing (Figure 2), with the highest correlation coefficient being was recorded at a certain record length. This result indicates that the most stable record length to monitor drought could be identified.

Correlation coefficient results on the monthly time scale suggested that the index having the highest correlation coefficient among all indices differed in different climate regions at different time scales. However, it was clear that the K and Pa indices were mostly recommended as having the highest correlation coefficient among all indices. SPEI and HI indices recorded high stability, indicating that different lengths of record had less influence on them on monthly time scales in different climate regions. In this scale, the GEVI index predominantly had the lowest correlation coefficient among all indices, recording a weak correlation in some lengths of the record, suggesting that that GEVI index was heavily affected by record length on the monthly time scale (Figure 3). However, the correlation coefficient of almost all indices was greater than 0.91, except for GEVI (0.54 to 0.99 range).

At the seasonal time scale, more obvious differences in correlation coefficient results were recorded between the indices. As per the monthly scale, the GEVI index also has the lowest correlation coefficient among all indices, and it was significantly reduced for the lowest GEVI index (0.30), resulting in a weak relationship between them in some of the record lengths (Figure 3). On this scale, K, Pa and SPEI indices recorded the

highest correlation coefficients in different climate regions, and the correlation coefficient of almost all indices was higher than 0.92 (except for GEVI).

Correlation coefficient results obtained on the annual time scale were similar to those recorded on the seasonal time scale; correlation coefficient results in the GEVI index were also significantly reduced compared with the seasonal time scale. On this scale, indices predominantly having the highest correlation coefficient included K and Pa indices; SPEI and SPI indices had high correlation coefficients in different climatic regions. In all studied stations, correlation coefficients between records were greater than 0.99, and correlation coefficients expressed an increasing trend as the time scale increased.

4.2. Comparison of match and non-match in the studied indices

Investigating match and non-match of different drought classes for all time scales derived from all record periods enabled applicability of indices at a region to be calculated. Match and non-match were determined using the following criteria: if one class of drought occurrence derived from *a* (30-57 years) lengths of record matched with *b* (also 30-57 years) lengths of record, it was termed as a match; if records did not match they were then termed as non-match. In this investigation, data for *a* and *b* were selected from 1988-2017, spanning the last 30 years. The percentage of non-match was obtained by dividing the number of "non-matches" into the sum of the number of "matches" and "non-matches". Despite dividing drought into four types, a number of extreme values were recorded for each class during this process, resulting in this analysis not fully reflect general characteristics. Therefore, we mainly discussed the total non-match of four non-matches, with the total percentage of non-match being obtained by dividing the sum of "non-matches" of the four classes into the sum of the number of "matches" and "non-matches" of the classes. Our results provided a 28×28 non-match matrix for a drought index at certain time scale when data was calculated for a station.

Firstly, by analyzing the percentages of non-match of the GEVI index on a monthly time scale for station A and B, we identified a block rule showing that the whole heatmap was divided into four blocks (Figure 4). It can be seen that the top left block and the bottom right block had a comparatively higher percentage of non-match, and the top right block and bottom left block had a comparatively lower percentage of non-match. This result enabled us to identify an optimal record length that had the lowest total percentage from all record lengths. However, different characteristics for the same drought index at different stations were identified. For example, the percentages of the GEVI index on the monthly time scale at station B were relatively lower when the length of record was less than 42 years, indicating that the same index had different applicability for different stations.

Based on our results, we identified a record length that had the lowest average percentage, termed as the optimal record length. We then calculated all optimal lengths at all stations, as well as obtaining their frequencies of occurrence. The frequency of optimal length for all stations was obtained for all indices. Results from this analysis indicated that the majority of optimal lengths from all stations to calculate drought indices was 41-45 years, with some indices at different time scales being 36-40 years and 46-50 years. However, K, Pa and SPI indices had relatively large differences among different frequencies of optimal length. Results also indicate that the frequency of optimal length initially increased before decreasing with an increase in record length for all indices at all time scales (Figure 5).

Results for the GEVI index indicated that record lengths of 36-40 years and 41-45 years had the highest frequency among all record lengths on the monthly time scale; the record length of 36-45 years was the optimal length for the GEVI index on the monthly time scale. On seasonal and annual time scales, the record length of 41-45 years also recorded the highest frequency.

346 The optimal record length for the HI index was 41-45 years on the monthly and seasonal time scale. Record
347 lengths of 36-40 and 46-50 years were very close to the optimal record length on the seasonal time scale,
348 indicating that optimal record lengths on the seasonal timescale were 36-50 years. In addition, frequencies of
349 36-40, 41-45, 46-50 and 51-57 years were very close to each other on the annual time scale, indicating that there
350 were no obviously optimal record lengths for the HI index on the annual time scale.
351 Results for the K index also indicated optimal record lengths of 46-50 years on the monthly and seasonal
352 time scales. On the annual time scale, 40-45 and 46-50 years were shown to be optimal, suggesting that the
353 overall optimal record length was 40-50 years. Similar results were also recorded for the Pa index, with 41-45
354 years being the optimal record length on the monthly and seasonal time scales; the optimal record length on the
355 annual time scale was 46-50 years.
356 In terms of SPEI and SPI indices, 41-45 years were the optimal record lengths on the monthly, seasonal and
357 annual time scales. The frequencies of 36-40 years and 46-50 years were very close to that of the 41-45 year
358 record length for the SPEI index on the monthly time scale, and the frequency of 36-40 year record length was
359 very close to that of the 41-45 year record for the SPEI index at seasonal time scale.
360 On the CZI index, record lengths of 36-40 years and 41-45 years had the highest frequency among all
361 record lengths on the monthly time scale. For the seasonal and annual time scales, the 41-45 year record length
362 recorded the highest frequency.

363 4.3. Comparison of actual drought recognition rates of different indices on the seasonal
364 time scale

365 As statistical data used for the seasonal time scale was attainable, we evaluated the applicability of drought
366 indices on this time scale. For this analysis, based on historical drought and no-drought data from 1988-2016,

367 the actual drought and no-drought recognition rate (R) was obtained by dividing the sum of the number that the
368 drought index can recognize drought and no-drought into the sum of the number that suffered from drought and
369 no-drought events from 1988-2016.

370 By calculating R from all record lengths, results indicated that the HI index had the highest frequency of
371 max R at all record lengths, with SPEI and Pa indices also having high results (Figure 6). The lowest frequency
372 of the highest R value was recorded by the K index, with CZI and GEVI indices also having low frequencies.
373 Frequency results of max R calculated at different record lengths therefore, indicated that HI, SPEI and Pa
374 indices had better applicability for different regions; the K index recorded the lowest applicability. Results for
375 different climate zones of indices having the highest R are shown on Figure 6 and Table 3.

376 **5. Conclusions**

377 In order to analyze drought events in different countries, it is important to examine long-term data spanning
378 at least 30 years. Data collection at meteorological stations can also vary between stations, and between
379 countries. It is therefore difficult to select long enough lengths of record to calculate, and it can be from 30-year
380 data to the length being from the beginning of record to the present. The selected length of recording data cannot
381 be ignored due to drought indices changing with record length. In this investigation, we evaluated the sensitivity
382 of precipitation and evapotranspiration record lengths to identify the lowest impact values. This method can
383 account for selecting weak data, as well as the applicability of different drought indices at different regions.

384 On the three examined time scales, K, Pa and SPEI indices recorded better time stability compared to other
385 indices. As the time scale increased, the correlation coefficient of the indices also increased. These indices are
386 very stable at different record lengths for the different climatic zones of the study region. The GEVI index
387 recorded the lowest time stability compared to the other indices, recording a significant downward trend as the

388 time scale increased, indicating that the GEVI index had relatively low applicability. This indicated that indices
389 only derived from precipitation may have lower stability compared with precipitation-evapotranspiration-based
390 indices. The generalized extreme value distribution function of GEVI also had lower applicability for drought
391 monitoring compared with the gamma distribution function of SPI and the Pearson Type Ⅲ distribution
392 function of CZI. We therefore had to select an appropriate distribution function to describe regional
393 precipitation if only precipitation-based indices were used.

394 In addition, we found that the majority of optimal record lengths for all stations had a lowest non-match of
395 41-45 years; some indices at different time scales also had a non-match for 36-40 years and 46-50 years. Results
396 for the K, Pa and SPI indices had relatively large differences among different frequencies for optimal length.
397 The percentage of non-match also reflected a trend of initially decreasing before increasing as the record length
398 increased, indicating that a kind of periodicity law at 57-year record lengths existed, whereby the non-match
399 percentage would reduce to the minimum at a certain record length.

400 As it was unknown if analyzing the characteristics of drought indices could identify actual drought events,
401 actual drought and no-drought recognition rates of different indices on the seasonal time scale were calculated.
402 Results indicated that the HI index had the highest actual drought recognition rate at almost all climate zones,
403 followed by the Pa and SPEI indices. According to results from this study, more priority can be given to
404 precipitation-evapotranspiration-based indices for regional drought monitoring.

405

406 **Acknowledgements**

407 This study was supported by the National Natural Science Foundation of China (Grant No.51879223) and
408 the National Key Research and Development Program of China (Grant No.2016YFC0400201).

References

Adnan S, Ullah K, Shuanglin L, Gao S, Khan AH, Mahmood R (2017): Comparison of various drought indices to monitor drought status in Pakistan. Climate Dynamics 51, 1885-1899. https://doi.org/10.1007/s00382-017-3987-0

Afzal M, Ragab R (2020): Assessment of the potential impacts of climate change on the hydrology at catchment scale: modelling approach including prediction of future drought events using drought indices. 10(10). https://doi.org/10.1007/s13201-020-01293-1

Ahmadalipour A, Moradkhani H, Demirel MC (2017): A comparative assessment of projected meteorological and hydrological droughts: Elucidating the role of temperature. Journal of Hydrology, 553: 785-797. https://doi.org/10.1016/j.jhydrol.2017.08.047

Alam NM, Sharma GC, Moreira E, Jana C, Mishra PK, Sharma NK, Mandal D (2017): Evaluation of drought using SPEI drought class transitions and log-linear models for different agro-ecological regions of India. Physics and Chemistry of the Earth, Parts A/B/C, 100: 31-43. https://doi.org/10.1016/j.pce.2017.02.008

Amirataee B, Montaseri M, Rezaie H (2017): Regional analysis and derivation of copula-based drought Severity-Area-Frequency curve in Lake Urmia basin, Iran. J Environ Manage, 206: 134-144. https://doi.org/10.1016/j.jenvman.2017.10.027

Ayantobo OO, Li Y, Song S, Yao N (2017): Spatial comparability of drought characteristics and related return periods in mainland China over 1961–2013. Journal of Hydrology, 550: 549-567. https://doi.org/10.1016/j.jhydrol.2017.05.019

428 Begueria S, Vicente-Serrano SM, Reig F, Latorre B (2014): Standardized precipitation evapotranspiration index
429 (SPEI) revisited: parameter fitting, evapotranspiration models, tools, datasets and drought monitoring.
430 International Journal of Climatology, 34(10): 3001-3023. https://doi.org/10.1002/joc.3887
431 Chang J, Li Y, Wang Y, Yuan M (2016): Copula-based drought risk assessment combined with an integrated
432 index in the Wei River Basin, China. Journal of Hydrology, 540: 824-834.
433 https://doi.org/10.1016/j.jhydrol.2016.06.064
434 Dogan S, Berktay A, Singh VP (2012): Comparison of multi-monthly rainfall-based drought severity indices,
435 with application to semi-arid Konya closed basin, Turkey. Journal of Hydrology, 470-471: 255-268.
436 https://doi.org/10.1016/j.jhydrol.2012.09.003
437 Freire-González J, Decker C, Hall JW (2017): The Economic Impacts of Droughts: A Framework for Analysis.
438 Ecological Economics, 132: 196-204. https://doi.org/10.1016/j.ecolecon.2016.11.005
439 Geng Q, Wu P, Zhang Q, Zhao X, Wang Y (2014): Dry/wet climate zoning and delimitation of arid areas of
440 Northwest China based on a data-driven fashion. Journal of Arid Land, 6(3): 287-299.
441 https://doi.org/10.1007/s40333-013-0206-7
442 Hao C, Zhang J, Yao F (2015): Combination of multi-sensor remote sensing data for drought monitoring over
443 Southwest China. International Journal of Applied Earth Observation and Geoinformation, 35: 270-283.
444 https://doi.org/10.1016/j.jag.2014.09.011
445 Homdee T, Pongput K, Kanae S (2016): A comparative performance analysis of three standardized climatic
446 drought indices in the Chi River basin, Thailand. Agriculture and Natural Resources, 50(3): 211-219.
447 https://doi.org/10.1016/j.anres.2016.02.002

Huang B (1958): Preliminary draft of comprehensive natural regionalization in China. Acta Geographica Sinica, 24(4): 348-365.

Hui-Mean F, Yusop Z, Yusof F (2018): Drought analysis and water resource availability using standardised precipitation evapotranspiration index. Atmospheric Research, 201: 102-115. https://doi.org/10.1016/j.atmosres.2017.10.014

Jia B, Wang Y, Xie Z (2018): Responses of the terrestrial carbon cycle to drought over China: Modeling sensitivities of the interactive nitrogen and dynamic vegetation. Ecological Modelling, 368: 52-68. https://doi.org/10.1016/j.ecolmodel.2017.11.009

Kassaye AY, Shao G, Wang X, Wu S (2020): Quantification of drought severity change in Ethiopia during 1952–2017. Environment, Development and Sustainability. https://doi.org/10.1007/s10668-020-00805-y

Keyantash J, Dracup JA (2002): The Quantification of Drought: An Evaluation of Drought Indices. Bulletin of the American Meteorological Society, 83(8): 1167-1180.

Kim D-W, Byun H-R, Choi K-S (2009): Evaluation, modification, and application of the Effective Drought Index to 200-Year drought climatology of Seoul, Korea. Journal of Hydrology, 378(1-2): 1-12. https://doi.org/10.1016/j.jhydrol.2009.08.021

Lei T, Feng J, Lv J, Wang J, Song H, Song W, Gao X (2020): Net Primary Productivity Loss under different drought levels in different grassland ecosystems. Journal of Environmental Management, 274. https://doi.org/10.1016/j.jenvman.2020.111144

Liu Y, Ren L, Hong Y, Zhu Y, Yang X, Yuan F, Jiang S (2016): Sensitivity analysis of standardization procedures in drought indices to varied input data selections. Journal of Hydrology, 538: 817-830. https://doi.org/10.1016/j.jhydrol.2016.04.073

Lopez-Nicolas A, Pulido-Velazquez M, Macian-Sorribes H (2017): Economic risk assessment of drought impacts on irrigated agriculture. Journal of Hydrology, 550: 580-589. https://doi.org/10.1016/j.jhydrol.2017.05.004

Lu J, Carbone GJ, Huang X, Lackstrom K, Gao P (2020): Mapping the sensitivity of agriculture to drought and estimating the effect of irrigation in the United States, 1950–2016. Agricultural and Forest Meteorology, 292-293. https://doi.org/10.1016/j.agrformet.2020.108124

Ma, H., Yan, D., Wong, B., Fang, H., Shi, X., 2013. Applicability of typical drought indexes in the Luanhe River Basin. Arid Zone Research, 30(4): 728-734.

Ma M, Ren L, Singh VP, Yang X, Yuan F, Jiang S (2014): New variants of the Palmer drought scheme capable of integrated utility. Journal of Hydrology, 519: 1108-1119. https://doi.org/10.1016/j.jhydrol.2014.08.041

Mahmoudi P, Rigi A, Miri Kamak M (2019): Evaluating the sensitivity of precipitation-based drought indices to different lengths of record. Journal of Hydrology, 579. https://doi.org/10.1016/j.jhydrol.2019.124181

Makokha GO, Wang L, Zhou J, Li X, Wang A, Wang G, Kuria D (2016): Quantitative drought monitoring in a typical cold river basin over Tibetan Plateau: An integration of meteorological, agricultural and hydrological droughts. Journal of Hydrology, 543: 782-795. https://doi.org/10.1016/j.jhydrol.2016.10.050

Mallya G, Tripathi S, Govindaraju RS (2015): Probabilistic drought classification using gamma mixture models. Journal of Hydrology, 526: 116-126. https://doi.org/10.1016/j.jhydrol.2014.11.008

Mallya G, Mishra V, Niyogi D, Tripathi S, Govindaraju RS (2016): Trends and variability of droughts over the Indian monsoon region. Weather and Climate Extremes, 12: 43-68. https://doi.org/10.1016/j.wace.2016.01.002

McKee TB, Doesken NJ, Kleist J (1993): The ralationship of drought frequency and duration to time scales. Eighth Conference on Applied Climatology, Anaheim, California: 17-22.

Mercado VD, Perez GC, Solomatine D, van Lanen HAJ (2016): Spatio-temporal Analysis of Hydrological Drought at Catchment Scale Using a Spatially-distributed Hydrological Model. Procedia Engineering, 154: 738-744. https://doi.org/10.1016/j.proeng.2016.07.577

Mishra AK, Singh VP (2010): A review of drought concepts. Journal of Hydrology, 391(1-2): 202-216. https://doi.org/10.1016/j.jhydrol.2010.07.012

Nam W-H, Hayes MJ, Svoboda MD, Tadesse T, Wilhite DA (2015): Drought hazard assessment in the context of climate change for South Korea. Agricultural Water Management, 160: 106-117. https://doi.org/10.1016/j.agwat.2015.06.029

Palmer WC (1965): Meteorological Drought. U.S. Department of Commerce Weather Bureau Research Paper.

Peña-Gallardo M, Vicente-Serrano SM, Domínguez-Castro F, Beguería S (2019): The impact of drought on the productivity of two 1 rainfed crops in Spain. Natural Hazards and Earth System Sciences, 1. https://doi.org/10.5194/nhess-2019-1

Quesada-Hernández LE, Calvo-Solano OD, Hidalgo HG, Pérez-Briceño PM, Alfaro EJ (2019): Dynamical delimitation of the Central American Dry Corridor (CADC) using drought indices and aridity values. Progress in Physical Geography: Earth and Environment, 43(5): 627-642. https://doi.org/10.1177/0309133319860224

Ribeiro AFS, Pires CAL (2016): Seasonal drought predictability in Portugal using statistical–dynamical techniques. Physics and Chemistry of the Earth, Parts A/B/C, 94: 155-166. https://doi.org/10.1016/j.pce.2015.04.003

510 Spinoni J, Naumann G, Vogt JV (2017): Pan-European seasonal trends and recent changes of drought frequency
511 and severity. Global and Planetary Change, 148: 113-130. https://doi.org/10.1016/j.gloplacha.2016.11.013
512 Stagge JH, Kohn I, Tallaksen LM, Stahl K (2015): Modeling drought impact occurrence based on
513 meteorological drought indices in Europe. Journal of Hydrology, 530: 37-50.
514 https://doi.org/10.1016/j.jhydrol.2015.09.039
515 Su B, Huang J, Fischer T, Wang Y, Kundzewicz ZW, Zhai J, Sun H, Wang A, Zeng X, Wang G, Tao H, Gemmer
516 M, Li X, Jiang T (2018): Drought losses in China might double between the 1.5 °C and 2.0 °C warming.
517 Proceedings of the National Academy of Sciences, 115(42): 10600-10605.
518 https://doi.org/10.1073/pnas.1802129115
519 Touma D, Ashfaq M, Nayak MA, Kao S-C, Diffenbaugh NS (2015): A multi-model and multi-index evaluation
520 of drought characteristics in the 21st century. Journal of Hydrology, 526: 196-207.
521 https://doi.org/10.1016/j.jhydrol.2014.12.011
522 Valverde-Arias O, Garrido A, Valencia JL, Tarquis AM (2017): Using geographical information system to
523 generate a drought risk map for rice cultivation: Case study in Babahoyo canton (Ecuador). Biosystems
524 Engineering. https://doi.org/10.1016/j.biosystemseng.2017.08.007
525 Vicente-Serrano SM, Beguería S, López-Moreno JI (2010): A Multiscalar Drought Index Sensitive to Global
526 Warming: The Standardized Precipitation Evapotranspiration Index. Journal of Climate, 23(7): 1696-1718.
527 https://doi.org/10.1175/2009jcli2909.1
528 Vicente-Serrano SM, Van der Schrier G, Beguería S, Azorin-Molina C, Lopez-Moreno J-I (2015): Contribution
529 of precipitation and reference evapotranspiration to drought indices under different climates. Journal of
530 Hydrology, 526: 42-54. https://doi.org/10.1016/j.jhydrol.2014.11.025

Vicente-Serrano SM, Quiring SM, Peña-Gallardo M, Yuan S, Domínguez-Castro F (2019): A review of environmental droughts: Increased risk under global warming? Earth-Science Reviews. https://doi.org/10.1016/j.earscirev.2019.102953

Wang W, Guo B, Zhang Y, Zhang L, Ji M, Xu Y, Zhang X, Zhang Y (2020): The sensitivity of the SPEI to potential evapotranspiration and precipitation at multiple timescales on the Huang-Huai-Hai Plain, China. Theoretical and Applied Climatology. https://doi.org/10.1007/s00704-020-03394-y

Wang Z, Wang J, Li Y, Wang C (2013): Comparison of application between Generalized Extreme Value Index and Standardized Precipitaion Index in Northwest China. Plateau Meteorology, 32(3): 839-847.

Wei J, Ma Z (2003): Comparison of Palmer Drought Severity Index, Percentage of Precipitation Anomaly and Surface Humid Index. Acta Geographica Sinica, 58: 117-124.

Wu H, Hayes MJ, Wilhite DA, Svoboda MD (2005): The effect of the length of record on the standardized precipitation index calculation. International Journal of Climatology, 25(4): 505-520. https://doi.org/10.1002/joc.1142

Wu J, Zhou L, Mo X, Zhou H, Zhang J, Jia R (2015): Drought monitoring and analysis in China based on the Integrated Surface Drought Index (ISDI). International Journal of Applied Earth Observation and Geoinformation, 41: 23-33. https://doi.org/10.1016/j.jag.2015.04.006

Wu Y, Shi Q, Chang S (2011): Characteristics of temperal and spatial distributions of the drought and flood in Xinjiang region from 1961 to 2008. Plateau Meteorology, 30(2): 391-396.

Wu Z, Zhan P, Chen Z, Fang Q (2012): Assessment of the rare drought event occurred in Anshun of Guizhou Province by three drought indexes. Journal of Arid Meteorology, 30(3): 315-322.

551 Xu K, Yang D, Yang H, Li Z, Qin Y, Shen Y (2015): Spatio-temporal variation of drought in China during 1961–
552 2012: A climatic perspective. Journal of Hydrology, 526: 253-264.
553 https://doi.org/10.1016/j.jhydrol.2014.09.047
554 Yao N, Li Y, Lei T, Peng L (2017): Drought evolution, severity and trends in mainland China over 1961-2013.
555 Sci Total Environ, 616-617: 73-89. HTTPS://DOI.ORG/10.1016/j.scitotenv.2017.10.327
556 Zhang Q, Kong D, Singh VP, Shi P (2017): Response of vegetation to different time-scales drought across China:
557 Spatiotemporal patterns, causes and implications. Global and Planetary Change, 152: 1-11.
558 https://doi.org/10.1016/j.gloplacha.2017.02.008
559 Zhao H, Gao G, An W, Zou X, Li H, Hou M (2017): Timescale differences between SC-PDSI and SPEI for
560 drought monitoring in China. Physics and Chemistry of the Earth, Parts A/B/C, 102: 48-58.
561 https://doi.org/10.1016/j.pce.2015.10.022
562 Zhou Z, Shi H, Fu Q, Li T, Gan TY, Liu S (2020): Assessing spatiotemporal characteristics of drought and its
563 effects on climate-induced yield of maize in Northeast China. Journal of Hydrology, 588.
564 https://doi.org/10.1016/j.jhydrol.2020.125097
565

The list of figure caption

Figure 1. Climatic classification of arid areas of Northwest China and the geographical position of the meteorological stations.

Figure 2. Correlation coefficient of all record lengths with all lengths at monthly time scale of K index in station A and Pa index in station B.

Figure 3. Correlation coefficient of all record lengths with all lengths at all time scales of different indices (1, 3 12 are monthly, seasonal and annual time scales, respectively).

Figure 4. General percentage of non-match on the GEVI index monthly time scale at station A and B.

Figure 5. Frequency of optimal record length for the lowest non-match of different indices at different time scales.

Figure 6. Spatial distribution of max actual drought recognition rate of different indices on the seasonal time scale at different record lengths.

580 **Figures**

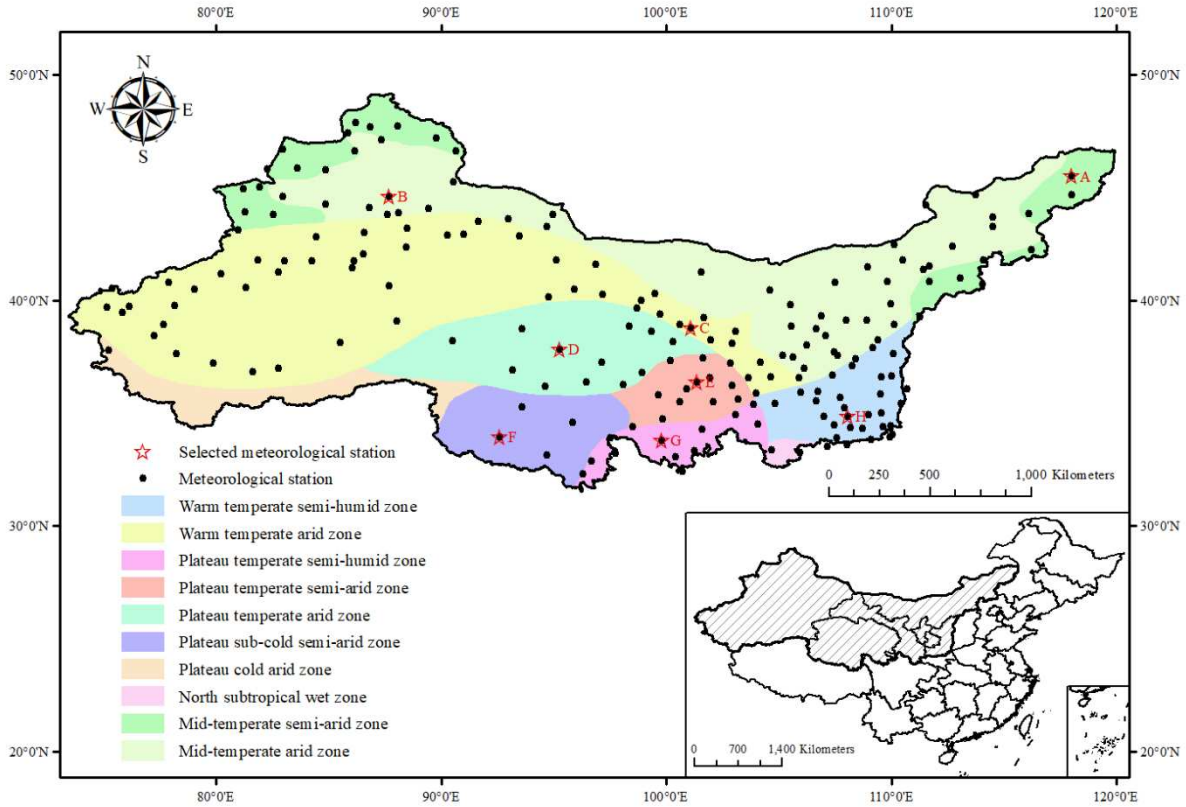

581

582 **Figure 1.** Climatic classification of arid areas of Northwest China and the geographical position of the

583 meteorological stations.

584

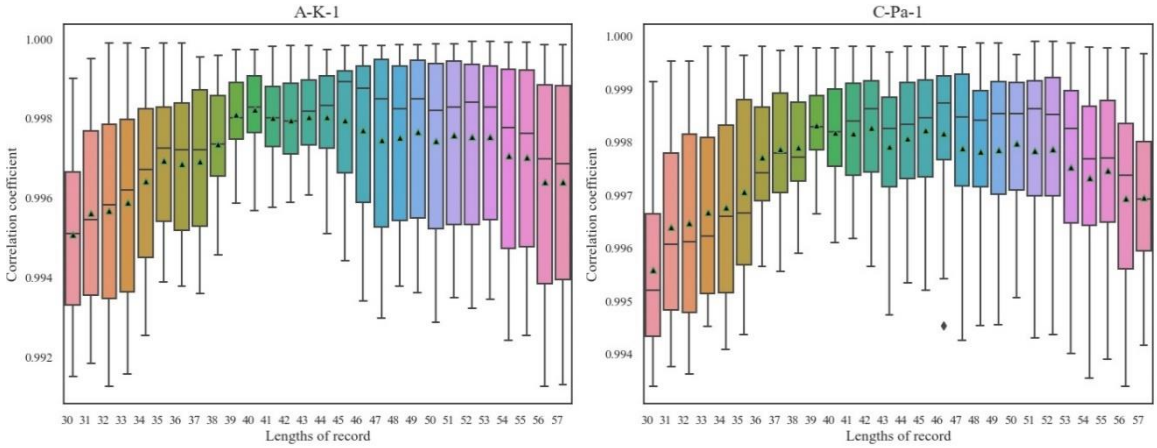

585

586 **Figure 2.** Correlation coefficient of all record lengths with all lengths at monthly time scale of K index in station

587 A and Pa index in station B.

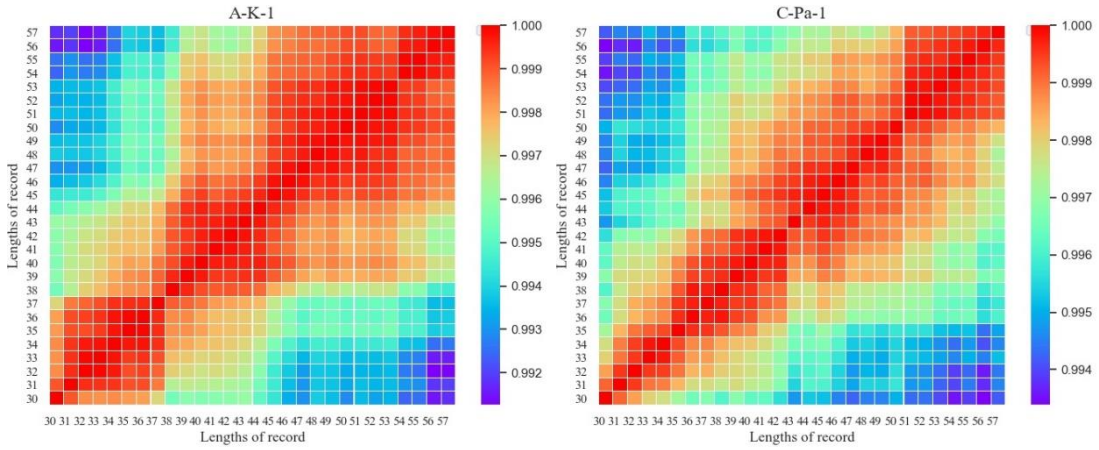
A-K-1
C-Pa-1
Lengths of record
Lengths of record

588

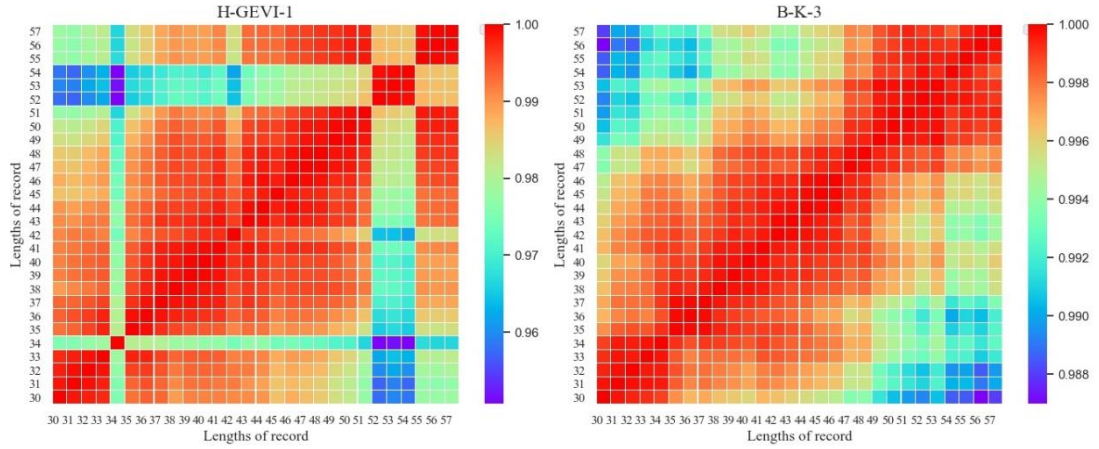
H-GEVI-1
B-K-3
Lengths of record
Lengths of record

589

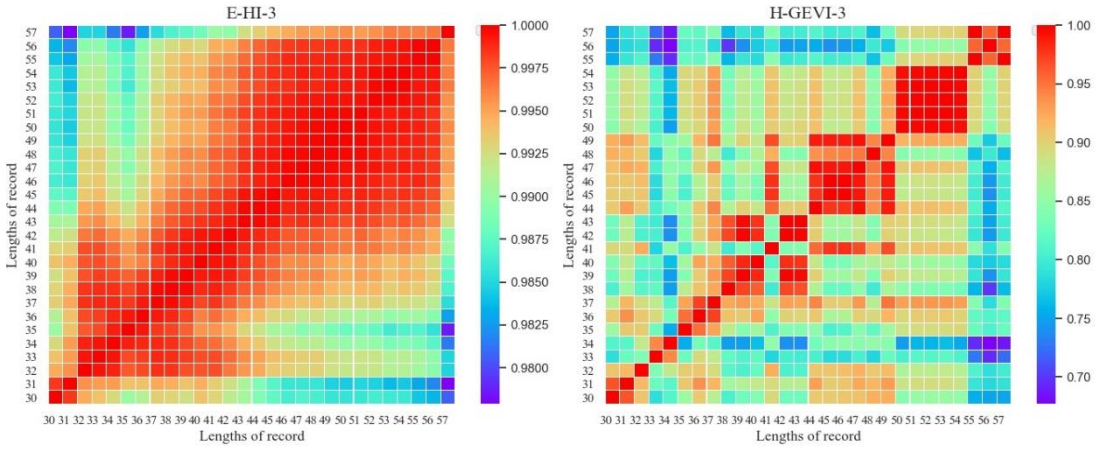
E-HI-3
H-GEVI-3
Lengths of record
Lengths of record

590

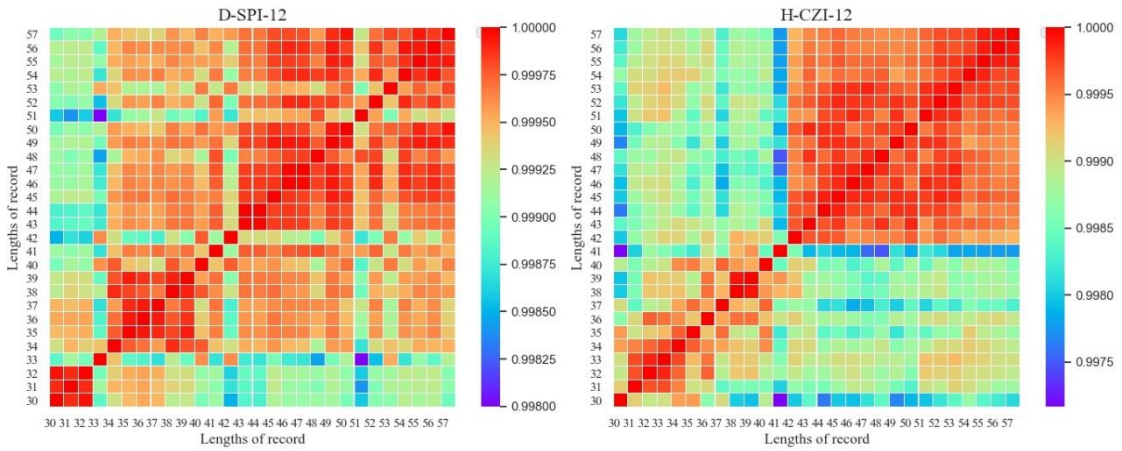

591

592 **Figure 3.** Correlation coefficient of all record lengths with all lengths at all time scales of different indices (1, 3

593 12 are monthly, seasonal and annual time scales, respectively).

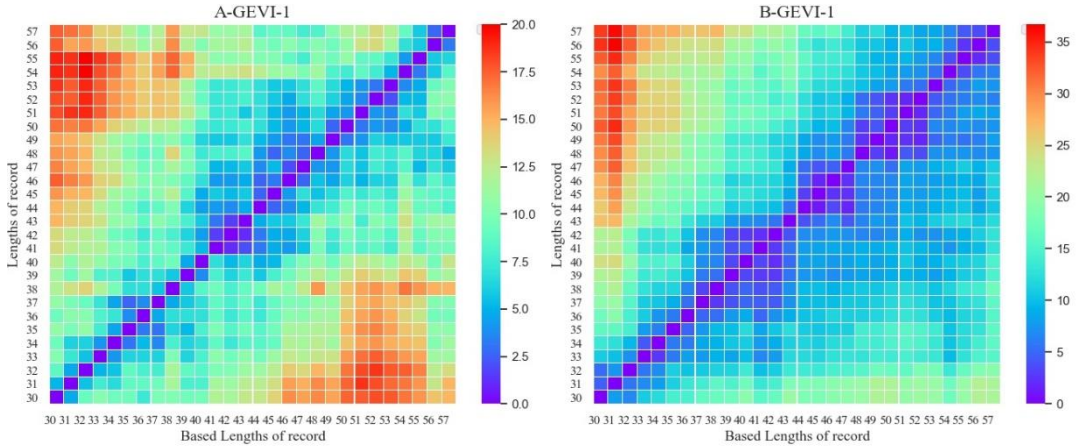

Figure 4. General percentage of non-match on the GEVI index monthly time scale at station A and B.

597

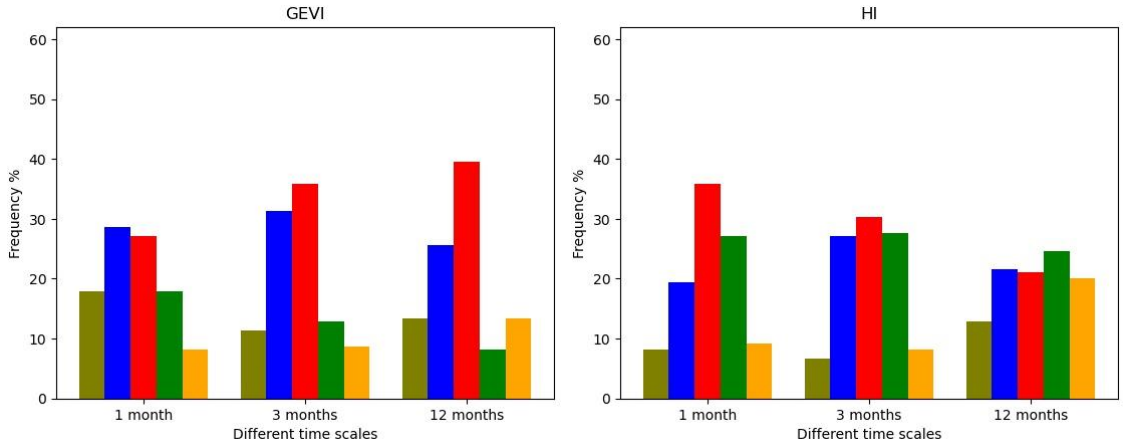

598

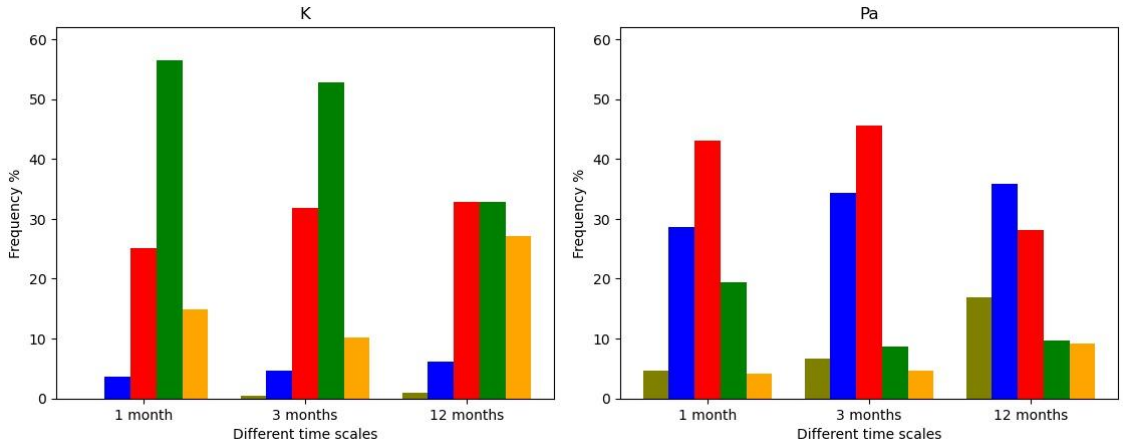

599

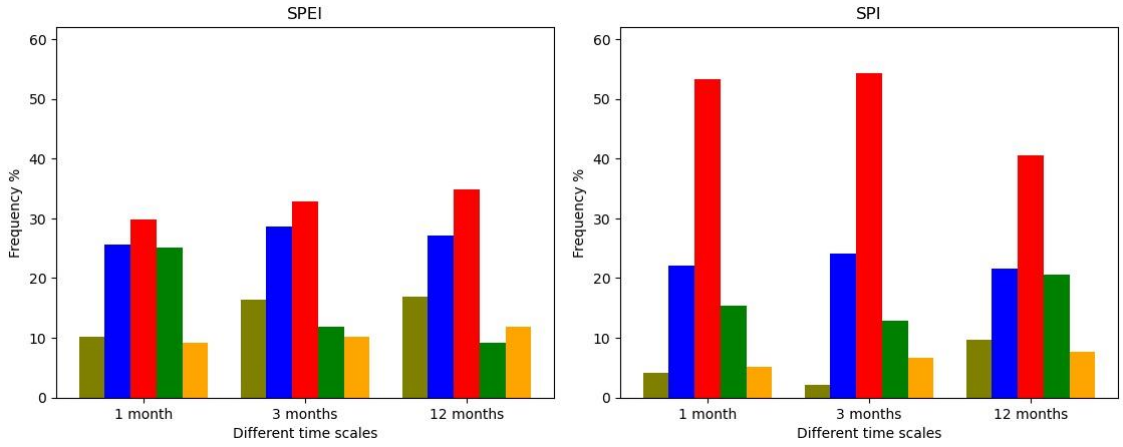

600

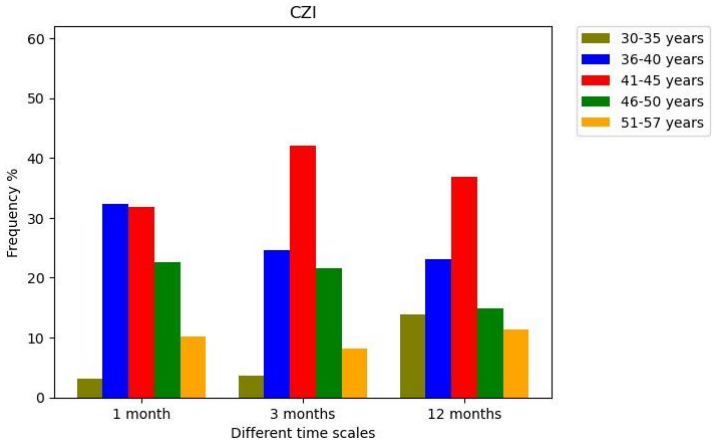

601

602 **Figure 5.** Frequency of optimal record length for the lowest non-match of different indices at different time

603 scales.

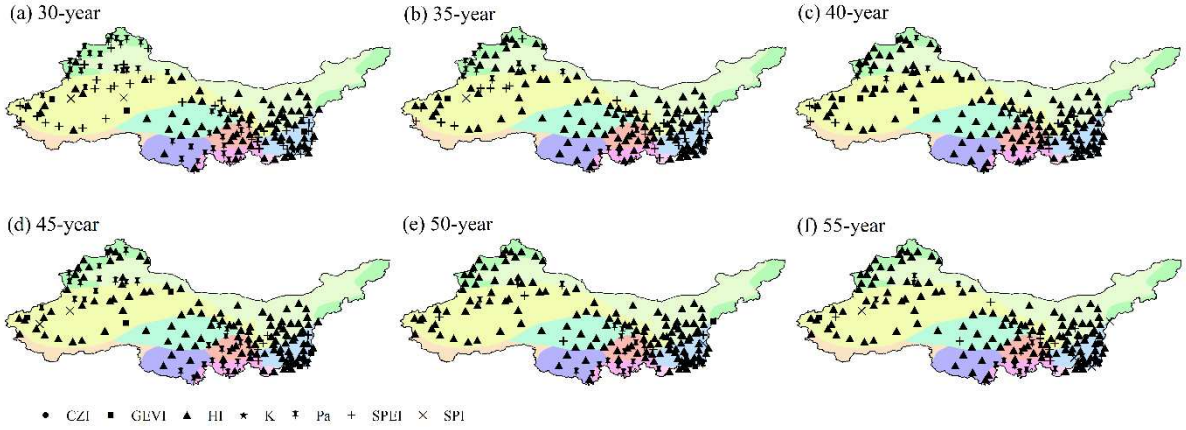

604

605 **Figure 6.** Spatial distribution of max actual drought recognition rate of different indices on the seasonal time

606 scale at different record lengths.

607

The list of table caption

Table 1. The names, geographical coordinates, annual average temperatures, average annual precipitation, year of station establishment and station type, 1988-2017.

Table 2 Classes of drought indices (Wet classes are not displayed).

Table 3. Drought indices of the highest actual drought recognition rates of different indices on the seasonal time scale at different climate zones.

Tables

Table 1. The names, geographical coordinates, annual average temperatures, average annual precipitation, year of station establishment and station type, 1988-2017.

Code	Station	Latitude	Longitude	Elevation (m)	Annual average temperature (℃)	Average annual precipitation (mm)	Year of station establishment	Station type
A	East Ujimqin	45.50°	118.00°	839.1	1.69	248.7	1955	Synoptic
B	Caijiahu	44.62°	87.70°	400	6.4	143.9	1958	Synoptic
C	Shandan	38.78°	101.08°	1795.5	6.78	203.6	1952	Synoptic
D	Da Qaidam	37.83°	95.28°	3000	2.16	91.2	1956	Synoptic
E	Guide	36.37°	101.37°	2211	7.6	256	1956	Synoptic
F	Tuotuo river	33.95°	92.62°	3050	-3.73	294.9	1956	Synoptic
G	Dari	33.80°	99.80°	4000	-0.64	555.5	1956	Synoptic
H	Yongshou	34.85°	108.05°	1330	11.22	581.9	1958	Synoptic

Table 2 Classes of drought indices (Wet classes are not displayed)

Value	Class	GEVI	HI	K	Monthly Pa/%	Seasonal Pa/%	Annual Pa/%	SPEI/SPI	CZI
1	Mild dry	-0.16 to -0.60	-0.85 to -1.60	1.0 to 0.8	-60 to -40	-50 to -25	-30 to -15	-0.5 to -1.0	0 to -0.84
2	Moderately dry	-0.60 to -1.00	-1.60 to -2.25	0.8 to 0.5	-80 to -60	-70 to -50	-40 to -30	-1.0 to -1.5	-0.84 to -1.44
3	Severely dry	-1.00 to -1.33	-2.25 to -2.80	0.5 to 0.2	-95 to -80	-80 to -70	-45 to -40	-1.5 to -2.0	-1.44 to -1.96
4	Extremely dry	⩽-1.33	⩽-2.80	⩽0.2	⩽-95	⩽-80	⩽-45	⩽-2.0	⩽-1.96

618 **Table 3.** Drought indices of the highest actual drought recognition rates of different indices on the seasonal time scale at different climate zones.

Different regions	30-year	35-year	40-year	45-year	50-year	55-year
mid-temperate semi-arid zone	Pa	HI, Pa	HI, Pa	HI, Pa	HI	HI
mid-temperate arid zone	HI, Pa	HI, SPEI, Pa	HI, SPEI	HI, Pa	HI	HI, Pa
warm temperate arid zone	HI, SPEI	HI, SPEI	HI, GEVI, SPEI	HI, Pa, GEVI	HI	HI, SPEI
plateau temperate arid zone	HI	HI	HI	HI, Pa	HI, Pa	HI
plateau sub-cold semi-arid zone	Pa	HI	HI	HI	HI	HI
plateau temperate semi-arid zone	HI, Pa	HI, Pa	HI	HI, Pa	HI, Pa	HI, Pa
plateau temperate semi-humid zone	HI, Pa	HI, SPEI	HI, Pa	HI, Pa	HI, Pa	HI, Pa
warm temperate semi-humid zone	HI, SPEI	HI, SPEI	HI	HI	HI, GEVI	HI

619